IEEE Access
Multidisciplinary | Rapid Review | Open Access Journal

Received 14 August 2022, accepted 7 September 2022, date of publication 12 September 2022, date of current version 21 September 2022.

Digital Object Identifier 10.1109/ACCESS.2022.3206380

RESEARCH ARTICLE

A Fast Parameter Identification Method for Composite Load Model Based on Jumping and Steady-State Points of Measured Data

YUJIE CHEN[1], HAO WU[1], (Member, IEEE), YIMING SHEN[1], XIAN MENG[2], AND PING JU[1], (Senior Member, IEEE)

[1]College of Electrical Engineering, Zhejiang University, Hangzhou, Zhejiang 310027, China
[2]Electric Power Research Institute of Yunnan Power Grid Company, Kunming, Yunnan 650217, China

Corresponding author: Hao Wu (zjuwuhao@zju.edu.cn)

This work was supported in part by the National Natural Science Foundation of China under Grant 51837004.

ABSTRACT The classic measurement-based method for load model parameter identification relies on lots of transient simulations and optimization iterations, which is computationally intensive, and is unsuitable to the terminal devices for recording load characteristic to participate in grid edge computing. To solve this difficulty, a fast identification method for load model parameters based on jumping and steady-state points of measured data is proposed, which greatly reduces the calculation time by avoiding the transient simulations and random optimizations of the classic method, and at the same time, well retains the accuracy of identified parameters. Firstly, the method extracts four points from measured data as calculation points, i.e., the point after voltage sag, two points before and after voltage recovery, and the final steady-state point. Then, the method calculates the state variables and powers at the four points through steady-state calculation, implicit trapezoid integration method and Hermite–Simpson method respectively. Finally, according to the measured powers of the four points, the method provides an initial key load model parameters through polynomial approximation method and finds the optimal parameters through Nelder-Mead algorithm. The accuracy and practicality of the method are demonstrated by test and field case studies, and the computation burden is less than 2.5% of that in the classic method without obvious loss of identification accuracy.

INDEX TERMS Load model parameter identification, jumping and steady-state points, Hermite–Simpson method, polynomial approximation, Nelder-Mead algorithm.

I. INTRODUCTION

Load model describes the relationship between load power and load voltage, which plays an important role in power system analysis, operation and control. It is well-known that an accurate load model contributes to reliable dynamic and static stability analysis, and hence has important influence on secure operation of power system. Therefore, the load model has received the attentions of many researchers in the past few decades, and various load structure and its typical parameters have been studied [1], [2], [3], [4]. However, the development of modern power system brings challenges to load modeling. On the one hand, the complexity and diversity of modern electrical loads are becoming increasingly prominent, which make that one set of typical parameters of load models are unsuitable for load modeling of whole power system, and call for accurate load model parameters for different types of typical loads [5], [6], [7]. On the other hand, the development of the renewable energy generation raises a new research topic about the generalized load modeling, which has received extensive attention in recent years [8].

The purpose of load modeling is to determine the model structure and its parameters which describe the response of load power with the load voltage changes. For the load model structure, the simplest and most commonly used one is the composite load model [9], i.e., induction motor paralleled with the static load, which has clearly physical meaning and can well reflect the dynamic and static characteristics

The associate editor coordinating the review of this manuscript and approving it for publication was Dong Shen.

of the load [10]. For determining the parameters, the component-based method and the measurement-based method are usually applied to load modeling in most researches. The component-based method establishes the load model based on the load composition and characteristic of individual components, which has a clear physical meaning [11], [12]. However, the complexity of modern electrical load requires a huge work on load composition and its components, making this method less used in nowadays. On the other hand, the measurement-based method identifies the load parameters based on field measured load data, without the need to know detail load information, and hence gets more and more practical application [13], [14].

The measurement-based method usually models the load model parameter identification as a parameter optimization problem. For a given set of measured load power and voltage, the method simulates load power under the given voltage with massive different load parameters, then searches the optimal load parameters to minimize the deviation between the simulated and measured powers using some heuristic methods. Usually, this method can offer quite accurate load parameters with less efforts comparing to the component-based method.

For the field measured data required by the measurement-based method, the dedicated load characteristic recording devices begin to be deployed in power system in recent years [15]. With the development of the edge computing in smart grid, computing resources of terminal equipment will become an important part of power grid operation and control in the future. Thus those recording devices are required to undertake the task of identifying parameters and uploading the results instead of complete data, which contributes to reduce the pressure of dispatch center and power communication network [16], [17], [18].

However, the classic measurement-based method needs to simulate load dynamic power under given load bus voltage disturbance, which is a high computation burden for the devices. At the same time, in order to find the optimal parameters, the heuristic methods usually use large populations and generations to avoid getting stuck in local optimum [19], which also increase the number of transient simulations by thousands, and makes the classic measurement-based method hard to be adopted in the devices.

Fast parameter identification method for load model with less computation burden is pursued by several researches in recent years. A fast online parameter identification and modeling method uses simplified composite load model to reduce computation, but this method can only identify the transient reactance of the motor and still needs transient simulation [20]. An imitation and transfer Q-learning-based identification approach is proposed to accelerate the identification rate and improve the identification accuracy by balancing greedy search and random global search, but this method still requires massive simulations and random search [21]. A two-step method for fast identification avoids transient simulations through 0+ method and multi-layer searching method, but can only identify specific parameters [22].

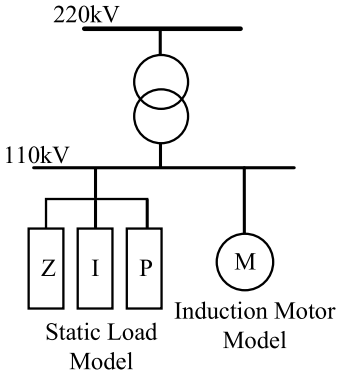

FIGURE 1. Composite load model with parallel connection of the static load model and the induction motor model.

A new fast parameter identification method for composite load model is proposed to apply in the load characteristic recording devices in this paper, which avoids simulating the powers at hundreds of sampling points and massive random optimizations in heuristic method. Specifically, only four jumping and steady-state points of the measured data, including one point after voltage sag, two points before and after voltage recovery, and one point corresponding to final steady-state, are extracted to approximately express the entire dynamic process. The state variables of the load model at final steady-state point are calculated by steady-state calculation, while those at the points after voltage sag and voltage recovery are calculated by the implicit trapezoidal method, and those at the point before voltage recovery are calculated by Hermite–Simpson method [23]. With the known state variables at the four points, their corresponding load powers can be easily calculated. Then, initial parameters are calculated by polynomial approximation method [24], and based on that, the optimal parameters are identified through Nelder-Mead algorithm [25]. The calculation process of this method is very simple compared with the classic measurement-based method, and hence the calculation time is less than 2.5% of that in the classic method with similar identification accuracy.

This paper is organized in the following way. Section II introduces the classic measurement-based load modeling method. Section III presents the detail steps of the proposed method. Section IV and V give the test case studies and field case studies respectively. Section VI concludes the paper.

II. CLASSIC MEASUREMENT-BASED LOAD MODELING METHOD FOR COMPOSITE LOAD MODEL

A. COMPOSITE LOAD MODEL

The simplest common load model structure used in power system is the composite load model shown in Fig.1, which is composed of static and dynamic load in parallel [9]. Because the fluctuation of frequency in power system is usually small, the influence of system frequency on load is ignored.

The static load model usually presents its active power P_S and reactive power Q_S as polynomial functions of load bus

voltage U [9], i.e.,

$$\begin{cases} P_{\mathrm{S}} = P_{\mathrm{S0}}\left[p_z\left(\dfrac{U}{U_0}\right)^2 + p_i\left(\dfrac{U}{U_0}\right) + p_p\right] \\ Q_{\mathrm{S}} = Q_{\mathrm{S0}}\left[q_z\left(\dfrac{U}{U_0}\right)^2 + q_i\left(\dfrac{U}{U_0}\right) + q_p\right] \end{cases} \tag{1}$$

where P_{S0} and Q_{S0} represent the rated active and reactive powers respectively; p_z, p_i, p_p, q_z, q_i and q_p, which satisfy the constraint $p_z + p_i + p_p = 1$ and $q_z + q_i + q_p = 1$, are the load parameters for active and reactive powers respectively. Because the load parameters can be interpreted as the proportions of constant impedance load, constant current load and constant power load, they are usually called ZIP parameters.

The dynamic load is usually modeled as third-order electromechanical transient model of induction motor, which contains two differential equations for rotor voltage and one differential equation for rotor motion, that is

$$\begin{cases} \dfrac{\mathrm{d}E'_{\mathrm{d}}}{\mathrm{d}t} = -\dfrac{1}{T'_{\mathrm{d0}}}[E'_{\mathrm{d}} + (X - X')I_{\mathrm{d}}] + s\omega_{\mathrm{s}}E'_{\mathrm{q}} \\ \dfrac{\mathrm{d}E'_{\mathrm{q}}}{\mathrm{d}t} = -\dfrac{1}{T'_{\mathrm{d0}}}[E'_{\mathrm{q}} - (X - X')I_{\mathrm{q}}] - s\omega_{\mathrm{s}}E'_{\mathrm{d}} \\ T_{\mathrm{j}}\dfrac{\mathrm{d}s}{\mathrm{d}t} = T_{\mathrm{m}} - T_{\mathrm{e}} \end{cases} \tag{2}$$

where E'_{d} and E'_{q} are the d-axis and q-axis transient electromotive forces of the motor respectively, s is the slip of the rotor, ω_{s} is the synchronous speed of the stator, T_{j} is the inertia time constant of the rotor, I_{d} and I_{q} are the currents of the stator respectively.

The other symbols in (2) are functions of previous parameters or variables. Specifically, X' and X represents the transient and open-circuit reactance respectively, T'_{d0} is the time constant of the rotor circuit when the stator circuit is open, T_{m} and T_{e} are the mechanical and electromagnetic torques of the motor respectively. They can be calculated by

$$\begin{aligned} X' &= X_{\mathrm{s}} + X_{\mathrm{r}}X_{\mathrm{m}}/\left(X_{\mathrm{r}} + X_{\mathrm{m}}\right) \\ X &= X_{\mathrm{s}} + X_{\mathrm{m}} \\ T'_{\mathrm{d0}} &= \frac{X_{\mathrm{r}} + X_{\mathrm{m}}}{R_{\mathrm{r}}} \\ T_{\mathrm{e}} &= E'_{\mathrm{d}}I_{\mathrm{d}} + E'_{\mathrm{q}}I_{\mathrm{q}} \\ T_{\mathrm{m}} &= T_{\mathrm{m0}}[A(1-s)^2 + B(1-s) + C] \end{aligned} \tag{3}$$

where X_{s} is the leakage reactance of the stator, X_{r} and R_{r} are the leakage reactance and resistance of the rotor, X_{m} is the magnetizing reactance of the motor, T_{m0} is the steady-state mechanical torque, and A, B, C are the mechanical torque coefficients, satisfying the constraint of $A(1 - s_0)^2 + B(1 - s_0) + C = 1$, where s_0 is the initial slip of the rotor.

Besides (2), the third-order electromechanical transient model of induction motor also contains two algebraic equations for stator voltage, that is

$$\begin{cases} U_{\mathrm{d}} = R_{\mathrm{s}}I_{\mathrm{d}} - X'I_{\mathrm{q}} + E'_{\mathrm{d}} \\ U_{\mathrm{q}} = R_{\mathrm{s}}I_{\mathrm{q}} + X'I_{\mathrm{d}} + E'_{\mathrm{q}} \end{cases} \tag{4}$$

where, U_{d} and U_{q} are the voltage of the stator respectively, R_{s} is the resistance of the stator.

The E'_{d}, E'_{q}, and s in (2) are the three state variables of the electromechanical transient model, which reflect the dynamic characteristics of the load and directly determine the output power of induction motor. Once those state variables under the given voltage are known, the active power P_{M} and reactive power Q_{M} of induction motor can be calculated by

$$\begin{cases} P_{\mathrm{M}} = U_{\mathrm{d}}I_{\mathrm{d}} + U_{\mathrm{q}}I_{\mathrm{q}} \\ Q_{\mathrm{M}} = U_{\mathrm{q}}I_{\mathrm{d}} - U_{\mathrm{d}}I_{\mathrm{q}} \end{cases} \tag{5}$$

Combing (1) and (5), the total active power P_{L} and reactive power Q_{L} of the load can be calculated by

$$\begin{cases} P_{\mathrm{L}} = P_{\mathrm{S}} + P_{\mathrm{M}} \\ Q_{\mathrm{L}} = Q_{\mathrm{S}} + Q_{\mathrm{M}} \end{cases} \tag{6}$$

To quantify the active power proportion of induction motor in whole load, $P_{\mathrm{M}}/P_{\mathrm{L}}$ at steady-state is defined as induction motor ratio P_{per}, which is an important parameter of the load model.

B. LOAD MODEL PARAMETERS

For the above composite load model, there are 14 independent parameters to be determined, including four static load model parameters, i.e., p_z, p_i, q_z, q_i, and ten dynamic load model parameters, i.e., P_{per}, X_{s}, X_{r}, R_{s}, R_{r}, X_{m}, A, B, s_0, T_{j}.

However, if all parameters are to be identified, the accuracy of the identification may not be guaranteed, and at the same time, it will consume a lot of computing time [26]. Therefore, only some important parameters need to be identified, while others are fixed as their typical values.

It has been verified that the parameters of static load model have lower sensitivities compared with those of dynamic load model [26], while for the parameters of induction motor model, most researches indicate that X_{m}, X_{r}, R_{s}, T_{j}, A and B have less effects on the load power dynamic [26], [27]. Thus, P_{per}, s_0, X_{s} and R_{r} are chosen as key parameters to be identified in this paper.

C. PARAMETER IDENTIFICATION METHOD

The purpose of the classic measurement-based method is to find a set of key parameters to minimize the deviation between the simulated and measured powers under the given voltage, and the objective function can be described as

$$J = \sum_{k=1}^{N}\left[(P_c(k) - P_m(k))^2 + (Q_c(k) - Q_m(k))^2\right] \tag{7}$$

where the P_c, Q_c, P_m, and Q_m are the simulated and measured powers respectively, N is the total sampling points.

Due to the complexity of the above optimization problem, the heuristic algorithms are usually used to identify the key parameters, such as, ant colony algorithm (ACO) [28], particle swarm algorithm (PSO) [28], genetic algorithm (GA) [29], and particle swarm-genetic hybrid algorithm (PSO-GA) [19].

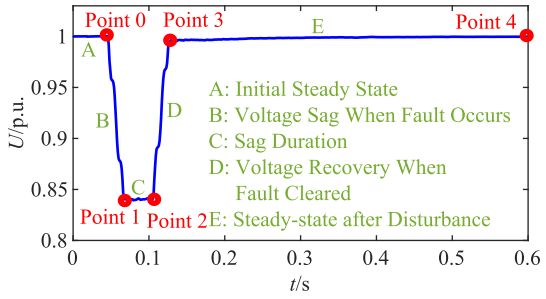

FIGURE 2. Illustration for extraction of point 0 to 4 from one typical voltage curve of the measured data.

However, when using heuristic algorithms, hundreds of iterations and thousands of transient simulations are usually required to find the optimal parameter values, which makes the classic measurement-based method cannot be adapt to load characteristic recording devices.

III. PARAMETER IDENTIFICATION METHOD BASED ON JUMPING AND STEADY-STATE POINTS

A. THE MOTIVATION OF THE PROPOSED METHOD

There are two main issues in the classic measurement-based method, which make it unsuitable to the devices. One is that the objective function needs to calculate the powers at each sampling point through transient simulation, which is time consuming. The other is that the optimization algorithm uses heuristics to find the optimal parameters, which require a large number of populations and iterations. To solve these issues, a new method is proposed in this paper.

1) OBJECTIVE FUNCTION

Take one typical voltage curve of the measured data shown in Fig. 2 as an example. It can be seen that four points, i.e., one point after voltage sag, two points before and after voltage recovery, and one point corresponding to final steady-state, can describe the key dynamic characteristics of the load approximately, which are denoted as point 1 to 4 respectively. Based on this observation, the optimization objective function in (7) can be simplified to the deviation between the calculated and measured powers of point 1 to 4, that is

$$J = \sum_{i=1}^{4} \left[\left(P_{c(i)} - P_{m(i)} \right)^2 + \left(Q_{c(i)} - Q_{m(i)} \right)^2 \right] \tag{8}$$

where, $P_{c(i)}$, $Q_{c(i)}$, $P_{m(i)}$, and $Q_{m(i)}$ are the calculated and measured powers of point i respectively. Besides the four points, the initial steady-state point before voltage sag is defined as point 0, which is crucial for calculating the powers of point 1 to 4.

For different field measured data, the occurrence and duration of the voltage sag can be different, so a method to determine the corresponding times of point 0 to 4 is needed, and the specific algorithm will be given in section III-B.

In order to calculate $P_{c(i)}$ and $Q_{c(i)}$ in (8), it is first necessary to solve the state variables of point 1 to 4. In section III-C, the state variables of point 1 to 4 will be calculated by steady-state initialization method, implicit trapezoidal method, and Hermite–Simpson method respectively instead of transient simulation.

2) OPTIMIZATION ALGORITHM

A two-stage identification algorithm is proposed in section III-D to find the optimal parameters of (8). In the first stage, the algorithm approximates the powers of point 1 to 4 as polynomial functions of load parameters, and transforms (8) into an explicit equation of the parameters to be identified. By directly solving the explicit equation, the initial parameters can be obtained. In the second stage, the Nelder-Mead algorithm is used to iteratively find the optimal parameters based on the initial parameters.

This algorithm uses dozens of direct search to avoid massive random search, and hence needs less iterations and computation burden compared with the heuristics used in the classic method.

B. DETERMINATION THE CORRESPONDING TIMES OF POINT 0 TO 4

The problem of determining the corresponding times of point 0 to 3 can be regarded as change-point detection problem of voltage curve. As shown in Fig. 2, the curve can be divided into five parts by point 0 to 3, whose corresponding times are T_1 to T_4 respectively.

For convenience, define the voltage derivative as U', the average value of U' in each part as $\bar{U}'$. Taking the part B as an example, it can be seen that U' is almost constant, so $\sum_{T_1}^{T_2} \left[U'(t) - \bar{U}' \right]^2$ in part B is also quite small, and the other parts are similar. Thus, the sum of the deviation squares between U' and $\bar{U}'$ of each part can be used as optimization target, and its mathematical model is described as

$$\begin{aligned} \min Y &= \sum_{i=1}^{5} \sum_{t=T_{i-1}}^{T_i} \left[U'(t) - \bar{U}'_i \right]^2 \\ s.t. &\begin{cases} U'(t) = \dfrac{U(t+\Delta t) - U(t)}{\Delta t} \\ \bar{U}'_i = \dfrac{T_i - T_{i-1}}{\Delta t} \displaystyle\sum_{t=T_{i-1}}^{T_i} U'(t) \\ 0 = T_0 < T_1 < \cdots < T_i < \cdots < T_5 \end{cases} \end{aligned} \tag{9}$$

where Δt is the sampling step, T_0 and T_5 are the start and end times of the measured data respectively.

T_1 to T_4 can be easily determined by pruned exact linear time method [30], which are the corresponding times of point 0 to 3.

As for point 4, its corresponding time will be set to T_5 directly, because this point can be considered as the final steady-state after the dynamic process.

C. CALCULATION STATE VARIABLES OF POINT 0 TO 4

1) POINT 0 AND POINT 4

Point 0 is the initial steady-state point, so the differential parts of (2) at point 0 are zero based on the steady-state condition.

Therefore, the state variables of point 0 can be calculated by (10) using the steady-state initialization method of induction motor.

$$\begin{cases} 0 = -\dfrac{1}{T'_{d0}}[E'_{d(0)} + (X - X')I_{d(0)}] + s_{(0)}\omega_s E'_{q(0)} \\ 0 = -\dfrac{1}{T'_{d0}}[E'_{q(0)} - (X - X')I_{q(0)}] - s_{(0)}\omega_s E'_{d(0)} \\ 0 = T_{m(0)} - T_{e(0)} \end{cases} \tag{10}$$

Point 4 is regarded as the final steady-state point of the measured data, and its state variables usually change very slowly over time, which can be approximated as constant. Thus the state variables of point 4 can be calculated in the same way as point 0.

2) POINT 1 AND POINT 3

Point 1 and point 3 are the jumping points of the measured data. Ideally, the state variables of point 1 and point 3 can be approximately considered as those of point 0 and point 2 due to the voltage sag and voltage recovery are a short-time process. However, some field measured data reveal that the voltage sag may last more than 0.02s. Thus, the dynamic processes during voltage sag and voltage recovery are considered here, and the state variables at point 1 and point 3 are calculated by popular implicit trapezoidal method, i.e.,

$$x_{k+1} - x_k = \frac{h_k}{2}(f_k + f_{k+1}) \tag{11}$$

Applying (11) to (2), the differential equations of induction motor are converted to algebraic equations. With known state variables of point 0, the state variables of point 1 can be obtained by solving

$$\begin{cases} E'_{d(1)} = E'_{d(0)} + \dfrac{t_{01}}{2}\{s_{(0)}\omega_s E'_{q(0)} + s_{(1)}\omega_s E'_{q(1)} \\ \quad - \dfrac{1}{T'_{d0}}[E'_{d(0)} + (X - X')I_{d(0)}] \\ \quad - \dfrac{1}{T'_{d0}}[E'_{d(1)} + (X - X')I_{d(1)}]\} \\ E'_{q(1)} = E'_{q(0)} + \dfrac{t_{01}}{2}\{-s_{(0)}\omega_s E'_{d(0)} - s_{(1)}\omega_s E'_{d(1)} \\ \quad - \dfrac{1}{T'_{d0}}[E'_{q(0)} - (X - X')I_{d(0)}] \\ \quad - \dfrac{1}{T'_{d0}}[E'_{q(1)} - (X - X')I_{d(1)}]\} \\ s_{(1)} = s_{(0)} + \dfrac{t_{01}}{2}\dfrac{1}{T_j}(T_{m(0)} - T_{e(0)} \\ \quad + T_{m(1)} - T_{e(1)}) \end{cases} \tag{12}$$

where, t_{01} is the time interval between point 0 and point 1.

The state variables of point 3 can be calculated in the same way after knowing the state variables of point 2.

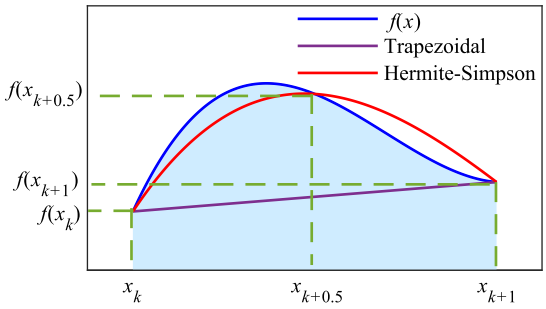

FIGURE 3. Schematic diagram of the Trapezoidal and Hermite–Simpson methods.

3) POINT 2

In most cases, the duration of voltage sag between point 1 and point 2 is more than 0.04s, which leads a remarkable change of state variables. Therefore, the state variables calculated by large-step implicit trapezoidal method have notable errors. Because of this, more accurate Hermite–Simpson method is used to calculate the state variables of point 2.

As shown in Fig. 3, the Hermite–Simpson method approximates the system dynamic as quadratic function, while the implicit trapezoidal method approximates that as linear function [23]. Therefore, when the step size is large, the Hermite–Simpson method is much more accurate than the implicit trapezoidal method. Thus, the Hermite–Simpson method is more suitable for the change trajectory of the state variables between point 1 and point 2, and only adds a small amount of computation burden compared with the implicit trapezoidal method.

In Hermite–Simpson method, x_{k+1} can be calculated by (13), which increases the $f_{k+0.5}$ term compared with (11), and the change of state variables between the x_k and x_{k+1} is transformed to Simpson quadrature from continuous integral [23].

$$x_{k+1} - x_k = \frac{h_k}{6}(f_k + 4f_{k+0.5} + f_{k+1}) \tag{13}$$

However, (13) cannot be directly applied to solve the state variables of point 2, because $f_{k+0.5}$ is a function of the extra state variable $x_{k+0.5}$, which are unknown. Therefore, a second collocation equation shown in (14) is used to calculate $x_{k+0.5}$ by constructing an interpolation [23].

$$x_{k+0.5} = \frac{1}{2}(x_k + x_{k+1}) + \frac{h_k}{8}(f_k - f_{k+1}) \tag{14}$$

Applying (13) and (14) to (2), the state variables of point 2 can be calculated by solving

$$\begin{aligned} \mathbf{x}_{(1.5)} &= \frac{1}{2}\left[\mathbf{x}_{(1)} + \mathbf{x}_{(2)}\right] + \frac{t_{12}}{8}\left[\mathbf{F}(\mathbf{x}_{(1)}) - \mathbf{F}(\mathbf{x}_{(2)})\right] \\ \mathbf{x}_{(2)} &= \mathbf{x}_{(1)} + \frac{t_{12}}{6}\left[\mathbf{F}(\mathbf{x}_{(1)}) + 4\mathbf{F}(\mathbf{x}_{(1.5)}) + \mathbf{F}(\mathbf{x}_{(2)})\right] \end{aligned} \tag{15}$$

where, $\mathbf{x} = \left[E'_d, E'_q, s\right]^T$ represents the state variables of the points, t_{12} is the time interval between point 1 and point 2, $\mathbf{F}$ represents the right hand sides of the differential equations

in (2), which can be describes as (16).

$$\mathbf{F}=\begin{bmatrix}-\frac{1}{T'_{\mathrm{d0}}}\left[E'_{\mathrm{d}}+(X-X')I_{\mathrm{d}}\right]+s\omega_{\mathrm{s}}E'_{\mathrm{q}}\\ -\frac{1}{T'_{\mathrm{d0}}}\left[E'_{\mathrm{q}}+(X-X')I_{\mathrm{q}}\right]+s\omega_{\mathrm{s}}E'_{\mathrm{d}}\\ \frac{1}{T_{\mathrm{j}}}\left(T_{\mathrm{m}}-T_{\mathrm{e}}\right)\end{bmatrix} \tag{16}$$

D. TWO-STAGE IDENTIFICATION ALGORITHM FOR LOAD MODEL PARAMETERS

A two-stage identification algorithm with less computation burden is proposed to find optimal parameters of the load model, which can minimize the optimization objective in (8). In the first stage, the algorithm obtains an approximate solution as initial parameters, and in the second stage, the initial parameters will be refined to obtain the optimal parameters.

1) CALCULATE INITIAL PARAMETERS BASED ON POLYNOMIAL APPROXIMATION

Polynomial approximation method can be used to obtain a simple polynomial function that approximates a complex relationship between inputs and output of a model, which is one of the state-of-art technique in power system analysis and control [24], [31], [32].

For the underlying parameter identification problem, this method is adopted to obtain explicit polynomial functions, which approximately describe the implicit relationship between the powers at point 1 to 4 and the parameters $\mathbf{p}$ to be identified. Then, substitute those explicit functions into (8) to obtain an polynomial approximation function of the optimization objective, and the $\mathbf{p}$ that gets minimum value of the polynomial approximation function can be easily solved out, which serves as the initial parameters of load model.

Let the approximated polynomial function denoted as

$$S\left(\mathbf{p}\right)\approx\tilde{S}\left(\mathbf{p}\right)=\sum_{0\le|\mathbf{n}|\le l}c_{\mathbf{n}}\Phi_{\mathbf{n}}\left(\mathbf{p}\right) \tag{17}$$

where, S can represent $P_{c(i)}$ or $Q_{c(i)}$, $\tilde{S}\left(\mathbf{p}\right)$ is a polynomial approximation function, $\mathbf{n}=(n_1,\ldots,n_d)$ includes the orders of polynomial for each parameter, $|\mathbf{n}|=n_1+\ldots+n_d$, d is the number of the parameters to be identified, l is the order of the polynomial approximation, $c_{\mathbf{n}}$ is the basis function coefficient, $\Phi_n(\mathbf{p})$ is the basis function. The reason of using polynomial to approximate the powers at point 1 to 4 rather than the objective function (8) is to obtain a relatively accurate initial parameters with the same order of polynomial approximation.

Two fundamental issues of the polynomial approximation are to determine the basis function and its corresponding coefficients. The polynomial chaos theory uses orthogonal polynomials as the basis for polynomial approximation [33], and the basis function $\Phi_{\mathbf{n}}(\mathbf{p})$ is obtained by multiplying each univariate orthogonal polynomial $\phi_{i,n_i}(p_i)$, i.e.,

$$\Phi_{\mathbf{n}}(\mathbf{p})=\prod_{i=1}^{d}\phi_{i,n_i}(p_i) \tag{18}$$

The choice of $\phi_{i,n_i}(p_i)$ for each parameter p_i can be related to its probability distribution. For the general parameter interval, its probability distribution can be considered as uniform distribution, and its corresponding polynomial is Legendre polynomial [24].

For the polynomial coefficient $c_{\mathbf{n}}$, it can be calculated by (19) through collocation method based on sparse grid integration, which originates from orthogonal projection theory [34].

$$c_{\mathbf{n}}=\frac{1}{C}\sum_{m=1}^{M}b_m\Phi_{\mathbf{n}}(\mathbf{p}^{(m)})S(\mathbf{p}^{(m)}) \tag{19}$$

where, M is the total number of collocation points, $\mathbf{p}^{(m)}$ is the collocation point, b_m is the collocation point coefficient. $C=\langle\Phi_{\mathbf{n}}(\mathbf{p}),\Phi_{\mathbf{n}}(\mathbf{p})\rangle$ is a constant, where $\langle\cdot,\cdot\rangle$ is the inner product of any two functions. The detail selection method for collocation points can be found in [34], which is omitted here for simplicity.

Based on (17) to (19), the explicit power functions for the parameters to be identified at point 1 to 4 can be obtained, and the optimization objective in (8) can be also approximated in a polynomial form. It should be noted that the obtained polynomial function is a global approximation over the entire parameter variation region, rather than a local approximation at expansion point like Taylor expansion.

Therefore, the minimum value of (8) and the corresponding parameters can be easily obtained by the trust region method based on interior point [35]. However, due to the errors in polynomial approximation, the parameters solved by this method can only serve as initial parameters.

2) FIND OPTIMAL PARAMETERS BASED ON NELDER-MEAD ALGORITHM

Nelder-Mead algorithm is used here to refine the initial parameters, which can directly search the optimal value of a objective function based on function values without the need of derivative information [25]. This algorithm iteratively transforms and updates a geometry with $n+1$ vertices in a n-dimensional parameter space, which is called simplex, and finally converges to the optimal parameter value.

The dimension of the parameter space here is the number of the parameters to be identified d, and the initial vertices of the simplex are chosen as the initial parameters together with d collocation points, which are closest to the initial parameters, and those vertices are denoted as $\mathbf{v}_1,\mathbf{v}_2,\cdots,\mathbf{v}_{d+1}$.

At each iteration, the algorithm sorts the $d+1$ vertices according to its corresponding objective function values which are calculated by (8), and then performs appropriate operations on those vertices, such as reflection, expansion, contraction, and shrink [36], so that the simplex moves closer to the optimal parameters. A schematic diagram of these operations in 2-dimensional space is shown in Fig. 4.

The steps for each iteration of Nelder-Mead algorithm:

1) Sort. Calculate $J(\mathbf{v}_j)$ at each vertex and sort as $J(\mathbf{v}_1)\le J(\mathbf{v}_2)\le\cdots\le J(\mathbf{v}_{d+1})$, where J is the objective

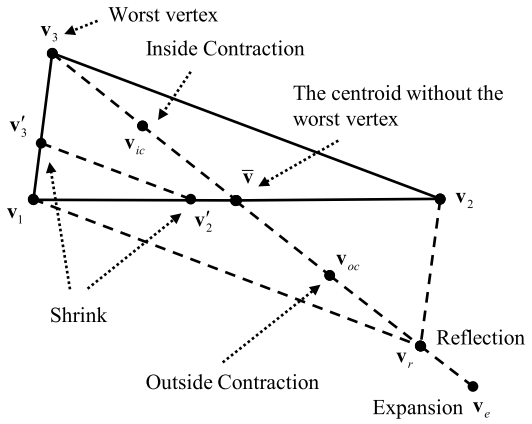

FIGURE 4. The reflection, expansion, contraction, and shrink operations of the Nelder-Mead algorithm in 2-dimensional space ($\mathbf{v}_1$, $\mathbf{v}_2$, and $\mathbf{v}_3$ are the simplex vertices, and $J(\mathbf{v}_1) \le J(\mathbf{v}_2) \le J(\mathbf{v}_3)$).

function in (8), $\mathbf{v}_{d+1}$ is the worst vertex, then calculate the centroid of the d best vertices $\bar{\mathbf{v}} = \frac{1}{d}\sum_{i=1}^{d}\mathbf{v}_i$.

2) Reflection. Calculate the reflection point $\mathbf{v}_r = \bar{\mathbf{v}} + \alpha(\bar{\mathbf{v}} - \mathbf{v}_{d+1})$, where α is reflection coefficient, usually as 1. If $J(\mathbf{v}_1) \le J(\mathbf{v}_r) < J(\mathbf{v}_d)$, replace $\mathbf{v}_{d+1}$ with $\mathbf{v}_r$.
3) Expansion. If $J(\mathbf{v}_r) < J(\mathbf{v}_1)$, then calculate the expansion point $\mathbf{v}_e = \bar{\mathbf{v}} + \beta(\mathbf{v}_r - \bar{\mathbf{v}})$, where β is expansion coefficient, satisfying $\beta > 1$. If $J(\mathbf{v}_e) < J(\mathbf{v}_r)$, replace $\mathbf{v}_{d+1}$ with $\mathbf{v}_e$, otherwise $\mathbf{v}_r$.
4) Outside contraction. If $J(\mathbf{v}_d) \le J(\mathbf{v}_r) < J(\mathbf{v}_{d+1})$, calculate the outside contraction point $\mathbf{v}_{oc} = \bar{\mathbf{v}} + \gamma(\mathbf{v}_r - \bar{\mathbf{v}})$, where γ is contraction coefficient, satisfying $0 < \gamma < 1$. If $J(\mathbf{v}_{oc}) \le J(\mathbf{v}_r)$, replace $\mathbf{v}_{d+1}$ with $\mathbf{v}_{oc}$, otherwise go to 6).
5) Inside contraction. If $J(\mathbf{v}_r) \ge J(\mathbf{v}_{d+1})$, calculate the inside contraction point $\mathbf{v}_{ic} = \bar{\mathbf{v}} - \gamma(\mathbf{v}_r - \bar{\mathbf{v}})$. If $J(\mathbf{v}_{ic}) < J(\mathbf{v}_{d+1})$, replace $\mathbf{v}_{d+1}$ with $\mathbf{v}_{ic}$, otherwise, go to 6).
6) Shrink. The simplex shrinks towards $\mathbf{v}_1$, i.e., $\mathbf{v}'_i = \mathbf{v}_1 + \delta(\mathbf{v}_i - \mathbf{v}_1)$, $i = 2, 3, \cdots, d+1$, where δ is shrink coefficient, satisfying $0 < \delta < 1$. Then, replace $\mathbf{v}_i$ with $\mathbf{v}'_i$.
7) Convergence Test. If $\left\{\frac{1}{d+1}\sum_{i=1}^{d+1}[J(\mathbf{v}_i) - J(\bar{\mathbf{v}})]^2\right\}^{\frac{1}{2}} \le \varepsilon$, where ε is the given precision, then output the optimal solution is $\mathbf{v}_1$, otherwise continue to iterate.

Based on the above steps of Nelder-Mead algorithm, the optimal parameters which can minimize (8) can be easily obtained through usually twenty iterations with the initial parameters.

E. THE STEP OF THE PROPOSED METHOD

Based on the simplified objective function (8), state variable calculation method and two-stage identification algorithm introduced in section III-A to III-D, the steps of the proposed fast parameter identification method for composite load model are as follows.

1) Input measured voltage and power; give the number and ranges of the parameters to be identified; set the polynomial approximation order.
2) Determine the corresponding times of point 0 to 4 based on the method in section III-B.
3) Calculate the collocation points for the given parameter ranges based on sparse grid integration [34].
4) Calculate the state variables of point 1 to 4 at collocation points based on (10), (12), and (16), then calculate the load powers at point 1 to 4 through (1) to (6).
5) Calculate basis function coefficient based on (19), then obtain the power explicit equations at point 1 to 4 as shown in (17).
6) Bring the power explicit equations into (8), and obtain the initial parameters by directly solving it.
7) Form a simplex with the initial parameters and d collection points which are closest to the initial parameters.
8) Perform appropriate operations and update the simplex based on section III-D2.
9) Repeat 8) until convergence, finally output the optimal parameters as identified parameters.

Based on the above steps, the identified parameters can be easily obtained. The accuracy of the identified parameters depends on the calculation errors of state variables at point 1 to 4 in section III-C, and the detailed accuracy analysis will be presented in section IV-A.

Compared to the classic measurement-based method, the proposed method accelerates the identification progress from the following two aspects:

1) The proposed method speeds up the calculation of state variables at point 1 to 4 through approximate calculation presented in section III-C, instead of the step-by-step transient simulation.
2) The proposed method uses a two-stage identification algorithm presented in section III-D, which reduces the scale of optimization, and hence speeds up the identification speed.

The detail computation burden of the proposed method will be analyzed in section IV-B.

IV. TEST CASE STUDY

A single-machine-infinite-bus system shown in Fig. 5 is built to verify the high accuracy, less computation burden and good robustness of the proposed method, where the load includes induction motor load and static load in polynomial form. The values of load parameters are shown in Table 1, which are the typical values for Chinese load model parameters.

A three-phase short circuit fault is set at 50% of the tie line at 0.1s, and then cleared at 0.2s. The voltage, active and reactive powers of the load are simulated for 1s with the step size of 0.001s, which are served as measured data for parameter identification of load model.

It has been pointed out in section II-B that P_{per}, s_0, X_{s}, and R_{r} have higher sensitivities to the dynamic process than the other parameters. Thus, in this paper, those parameters will

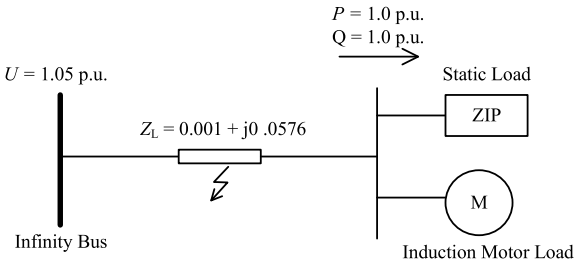

FIGURE 5. Single-machine-infinite-bus system where the load includes induction motor load and static load.

TABLE 1. The typical values of load model parameters.

	Parameter	Value	Parameter	Value
Parameters of Induction Motor Load	$\boldsymbol{P}_{\text{per}}$	**0.6**	$\boldsymbol{s}_0$	**0.0116**
	$\boldsymbol{X}_{\text{s}}$	**0.18**	$\boldsymbol{R}_{\text{r}}$	**0.02**
	R_{s}	0	X_{r}	0.12
	X_{m}	3.5	T_{j}	2
	A	0.85	B	0
Parameters of Static Load	p_z	1	p_i	0
	q_z	1	q_i	0

be identified, and the other parameters are fixed as typical values as shown in Table 1.

A. ACCURACY ANALYSIS

The accuracy of the proposed method is analyzed from two aspects. One is the calculation errors of state variables and powers at point 1 to 4, and the other is the relative errors of the identified parameters and the corresponding simulated powers.

1) STATE VARIABLES AND POWERS AT POINT 1 TO 4

For the given parameters in Table 1, the values of state variables and powers at point 1 to 4 are calculated by the method proposed in section III-C and transient simulation respectively, which are shown in Table 2.

The table also shows the relative errors between two methods. It can be seen from the table that the state variables calculated by proposed method have an error of less than 3%, and the powers have an error of less than 2%, indicating that the state variables and powers of point 1 to 4 are calculated quite accurately.

2) IDENTIFIED PARAMETERS AND THE CORRESPONDING SIMULATED POWERS

The two-stage algorithm for load model parameter identification proposed in section III-D is used to identify the key parameters from the measured data, and the identified parameters along with relative errors are shown in Table 3.

It can be seen from the table that the parameter with the largest relative error is X_{s}, whose error is 1.25%, and the relative errors of the other parameters are all less than

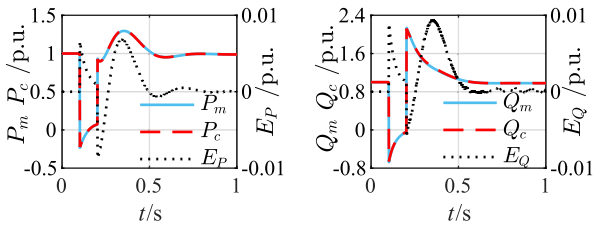

(a) Active power (b) Reactive power

FIGURE 6. Comparison between the measured and simulated powers, where P_m, Q_m, P_c, and Q_c are the measured and simulated powers respectively, E_P and E_Q are the absolute errors between the measured and simulated powers.

1%, indicating that the identified parameters of the proposed two-stage identification algorithm are quite accurate.

With the identified parameters, the active and reactive powers of the load can be simulated out, which are compared with the measured powers in Fig. 6. It can be seen from Fig. 6 that the simulated powers can well match the measured powers, and the absolute errors between simulated and measured powers are less than 0.01p.u..

In order to quantitatively evaluate the accuracy of the power curves, define the average power error indexes ε_P and ε_Q between the simulated and measured powers as (20), which are used to indirectly assess the accuracy of the identified parameters when the actual values of load parameters are unknown.

$$\varepsilon_P = \frac{1}{N}\sum_{k=1}^{N}\left|\frac{P_c(k)-P_m(k)}{P_m(k)}\right|$$
$$\varepsilon_Q = \frac{1}{N}\sum_{k=1}^{N}\left|\frac{Q_c(k)-Q_m(k)}{Q_m(k)}\right| \tag{20}$$

where, P_c, Q_c, P_m, and Q_m are the same as those of (7).

It can be figured out that the ε_P and ε_Q based on the identified parameters are 1.52% and 0.41% respectively, which shows that the simulated powers can well fit the measured powers, and also indirectly shows the accuracy of the identified parameters.

B. COMPUTATION BURDEN ANALYSIS

The computation burdens of the proposed method and the classic measurement-based load modeling method are compared in Table 4, where the classic method adopts the objective function (7), and uses particle swarm-genetic hybrid algorithm to identify the load model parameters, while the proposed method adopts the simplified objective function (8), and uses two-stage identification algorithm in section III-D. From Table 4, it can be seen that,

1) For the points needed in objective function, the proposed method requires only four points, i.e., point 1 to 4, while the classic method requires 1000 points.
2) For the calculation method of state variables, the proposed method uses a simpler direct calculation by (10),

TABLE 2. State variables and powers of point 1 to 4 calculated by the method proposed in section III-C and transient simulation.

	Point 1			Point 2			Point 3			Point 4		
	Proposed	Transient	Error	Proposed	Transient	Error	Proposed	Transient	Error	Proposed	Transient	Error
$E_d^{'}$	0.8646	0.8630	0.18%	0.1439	0.1414	1.80%	0.1442	0.1402	**2.86%**	0.8513	0.8513	0.00%
$E_q^{'}$	-0.1963	-0.1965	-0.10%	-0.2388	-0.2405	**-0.68%**	-0.2387	-0.2393	-0.27%	-0.1991	-0.1987	0.18%
s	0.0116	0.0117	-0.35%	0.0375	0.0376	-0.22%	0.0375	0.0378	**-0.64%**	0.0119	0.0119	0.18%
P	-0.2283	-0.2253	1.34%	0.0704	0.0715	**-1.62%**	0.9297	0.9293	0.04%	0.9887	0.9873	0.14%
Q	-0.6574	-0.6572	0.04%	-0.0415	-0.0417	**-0.36%**	2.1241	2.1246	-0.03%	0.9783	0.9785	-0.03%

TABLE 3. Comparison of the identified parameters with their actual values of the two-stage identification algorithm.

Parameter	Identified Value	Actual Value	Relative Error
P_{per}	0.6029	0.6	0.49%
s_0	0.01169	0.0116	0.81%
X_{s}	0.1778	0.18	**-1.25%**
R_{r}	0.0199	0.02	-0.50%

(12), and (16) instead of step-by-step transient simulation required by the classic method.

3) For the initial parameters calculation, the proposed method needs 4.75s to polynomial approximation of the powers at point 1 to 4, and 1.54s to solve the polynomial equation of objective function, which altogether takes 6.29s to obtain the initial parameters.
4) For the optimal parameters calculation, the proposed method has 5 vertices with 24 iterations, and requires to calculate the objective function for 216 times, which takes 2.38s. While the classic method has 30 populations with 50 iterations, and requires to calculate the objective function for 4500 times, which takes 375s. Obviously, the time needed by the proposed method is less than 1/100 of that needed by the classic method.
5) For the total calculation time, the proposed method spends 8.67s, which is less than 2.5% of 375s spent by the classic method.

Obviously, the proposed method has less computation burden and performs much faster compared with the classic method.

C. ROBUSTNESS ANALYSIS

The robustness of the proposed method is analyzed from the effect of the sampling error in the measured data. Fig. 7 shows the ε_P and ε_Q calculated based on the identified parameters of the measured data, which are superimposed with different sampling errors.

It can be seen from Fig. 7 that the power errors approximately linearly increase with the increase of the sampling errors. When the sampling error is less than 1%, the ε_P and ε_Q are less than 3.5% and 2% respectively, even if the sampling error reaches 2%, the power errors are still less than 5%.

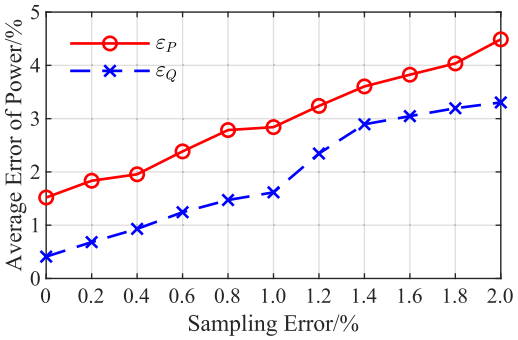

FIGURE 7. Average errors of active and reactive powers under the different sampling errors.

All of these show that the proposed method can maintain a well power fitting degree and good robustness in the face of sampling error.

Usually, the sampling error of the load characteristic recording devices is 0.2%. According to Fig. 7, the ε_P and ε_Q under this sampling error are 1.83% and 0.68% respectively. Therefore, the proposed method can fully meet the sampling accuracy of the devices.

V. FIELD CASE STUDY

Based on the field measured data recorded by load characteristic recording devices in 110kV outgoing lines of 220kV meshed power system, the practicality of the proposed method is analyzed. The field measured data are shown in Table 5, covering different voltage sag ratios, durations of voltage sag, and fault types. The proposed and classic methods are used for parameter identification from these field measured data respectively, and the key parameters to be identified are the same as those in section IV, with the other parameters fixed as typical values as shown in Table 1.

Taking fault 1 and 2 as examples, Fig. 8 shows the positions of the extracted point 0 to 3 in their measured voltage curves, where the positions of point 4 are not shown because their corresponding times exceed the maximal value of the horizon axis. It can been seen from Fig. 8 that the corresponding times of point 1 to 3 can be correctly determined by the method proposed in section III-B.

It should be noted that, the true values of load parameters for field measured data are unknown. Thus, the parameters identified by the classic method are served as benchmark

TABLE 4. Comparison of the computation burdens between the proposed and classic methods.

		Proposed Method	Classic Method
Points Needed in Objective Function		4 (point 1 to 4)	1000 (all sampling points)
Calculation Method of State Variables		direct calculation by (10), (12), (16)	step-by-step transient simulation
Initial Parameters Calculation	Time of Polynomial Approximation	4.75s	-
	Time of Solving Polynomial Equation of Objective Function	1.54s	-
Optimal Parameters Calculation	Number of Vertex/Population	5	30
	Iteration	24	50
	Number of Calculating Objective Function	216	4500
	Time	2.38s	375s
Total Calculation Time		**8.67s**	375s

TABLE 5. The field measured data in 110kV sub-transmission lines.

Fault	Line Name	Voltage sag ratio	Duration of Voltage Sag	Fault Type
1	LP Line	15.9%	0.038s	Single-phase Fault
2	XT Line	28.9%	0.12s	Three-phase Fault
3	LZ Line	5.8%	0.028s	Single-phase Fault
4	FH Line	20.7%	0.04s	Single-phase Fault
5	LT Line	21.2%	0.038s	Single-phase Fault

The voltage sag ratio is $(U_{\text{initial}} - \bar{U}_{\text{sag}})/U_{\text{initial}}$, where U_{initial} is the voltage amplitude before the sag, and $\bar{U}_{\text{sag}}$ is the average voltage amplitude during the sag.

TABLE 6. Average deviations and calculation times between the proposed and classic methods for all 5 faults.

Average Relative Deviation of Identified Parameter	P_{per}	7.85%
	s_0	6.91%
	X_{s}	5.08%
	R_{r}	8.19%
Average Calculation Time	Proposed	8.90s
	Classic	373s

values. Table 6 shows the average relative deviations of the identified parameters between the proposed and classic methods for all 5 faults, along with the calculation times of these two methods. It can be seen from Table 6 that,

1) The parameter with the largest average relative deviation is R_r, which is 8.19%. It shows that the identified parameters of the two methods are quite close.
2) The average calculation time of the proposed method is 8.90s, which is less than 2.5% of that of the classic method.

It should also be noted that the field measured data contain the true load powers. Thus the average values of ε_P and ε_Q

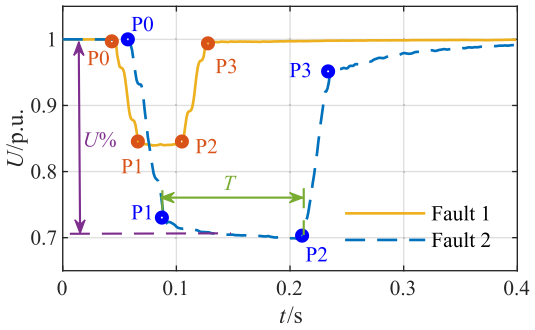

FIGURE 8. The positions of point 0 to 3 in voltage curves of fault 1 and 2, where P0 to P3 are the point 0 to 3, U% is the voltage sag ratio, T is the duration of voltage sag. Since the total durations of fault 1 and 2 are different, only the voltage curves of 0-0.4s are shown here.

TABLE 7. The average values of ε_P and ε_Q of the proposed and classic methods for all 5 faults.

	Average of ε_P	Average of ε_Q
Proposed Method	5.22%	11.12%
Classic Method	4.78%	10.14%
Deviation	0.45%	0.98%

of the proposed and classic methods for all 5 faults can be calculated directly, which are compared in Table 7. Besides, Fig. 9 and Fig. 10 compare the powers simulated by the identified parameters of the proposed and classic methods in fault 1 and 2 with respect to their corresponding measured powers. The Table 7, Fig. 9 and Fig. 10 show that,

1) The average values of ε_P and ε_Q of the proposed method for all 5 faults are 5.22% and 11.12% respectively, and the figures show that the simulated powers based on the identified parameters can well fit the measured powers in the field measured data.
2) The deviations between the average values of ε_P and ε_Q of the two methods are less than 1%, which shows that although the identified parameters between the

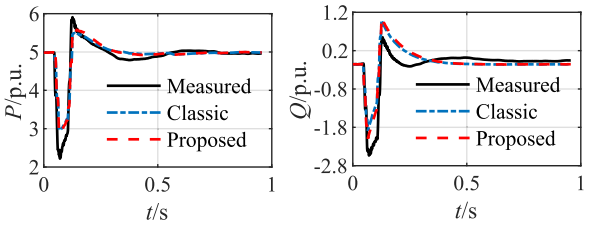

(a) Active power (b) Reactive power

FIGURE 9. Comparison between the powers simulated by the identified parameters of the proposed and classic methods with the measured powers in fault 1.

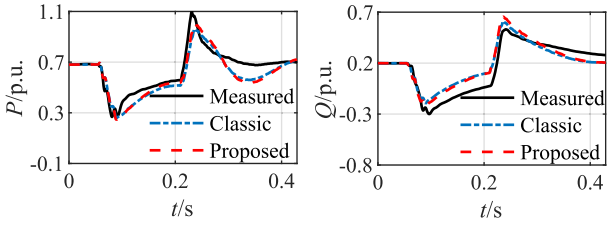

(a) Active power (b) Reactive power

FIGURE 10. Comparison between the powers simulated by the identified parameters of the proposed and classic methods with the measured powers in fault 2.

two methods have a deviation as large as 8.19%, the simulated powers of the two methods with respect to measured powers have similar errors.

In summary, the proposed method can maintain similar accuracy of the classic method, while has shorter computation time and good practicality in field measured data.

VI. CONCLUSION

A fast parameter identification method for composite load model based on jumping and steady-state points of the measured data is proposed in this paper, which adopts the following three unique techniques:

1) The four points, i.e., one point after voltage sag, two points before and after voltage recovery, and the final steady-state point, are extracted to approximately express the entire dynamic process and greatly simplify the objective function.
2) The three techniques, i.e., steady-state calculation, implicit trapezoid method and Hermite–Simpson method, are used to calculate the state variables of the four points directly, which greatly reduce the computation burden.
3) A two-stage identification algorithm, which adopts polynomial approximation method and Nelder-Mead algorithm to obtain initial parameters and optimal parameters respectively, is proposed to reduce the computation scale and time of the identification.

The test case studies show the proposed method has high accuracy, less computation burden and good robustness, while the field case studies show the proposed method has good practicality in field measured data, and hence the calculation time of the proposed method is less than 2.5% of that in the classic method without obvious loss of identification accuracy.

The further research direction of current work can be twofold. One is to research more flexible characteristic extraction method regarding voltage curve rather than the current four specific points. The other is to extend to the generalized load model so that disperse renewable energy generation can be considered in load model.

REFERENCES

[1] F. Bu, Z. Ma, Y. Yuan, and Z. Wang, "WECC composite load model parameter identification using evolutionary deep reinforcement learning," *IEEE Trans. Smart Grid*, vol. 11, no. 6, pp. 5407–5417, Nov. 2020.
[2] H. Bai, P. Zhang, and V. Ajjarapu, "A novel parameter identification approach via hybrid learning for aggregate load modeling," *IEEE Trans. Power Syst.*, vol. 24, no. 3, pp. 1145–1154, Aug. 2009.
[3] J. V. Milanovic, K. Yamashita, S. M. Villanueva, S. Ž. Djokic, and L. M. Korunović, "International industry practice on power system load modeling," *IEEE Trans. Power Syst.*, vol. 28, no. 3, pp. 3038–3046, Aug. 2013.
[4] X. Wang, Y. Wang, D. Shi, J. Wang, and Z. Wang, "Two-stage WECC composite load modeling: A double deep Q-learning networks approach," *IEEE Trans. Smart Grid*, vol. 11, no. 5, pp. 4331–4344, Sep. 2020.
[5] A. Arif, Z. Wang, J. Wang, B. Mather, H. Bashualdo, and D. Zhao, "Load modeling—A review," *IEEE Trans. Smart Grid*, vol. 9, no. 6, pp. 5986–5999, Nov. 2018.
[6] B.-K. Choi, H.-D. Chiang, Y. Li, H. Li, Y.-T. Chen, D.-H. Huang, and M. Lauby, "Measurement-based dynamic load models: Derivation, comparison, and validation," *IEEE Trans. Power Syst.*, vol. 21, no. 3, pp. 1276–1283, Aug. 2006.
[7] Z. Ma, Z. Wang, Y. Wang, R. Diao, and D. Shi, "Mathematical representation of WECC composite load model," *J. Modern Power Syst. Clean Energy*, vol. 8, no. 5, pp. 1015–1023, 2020.
[8] D. Xiao, H. Chen, C. Wei, and X. Bai, "Statistical measure for risk-seeking stochastic wind power offering strategies in electricity markets," *J. Modern Power Syst. Clean Energy*, early access, Dec. 8, 2021, doi: 10.35833/MPCE.2021.000218.
[9] H. Renmu, M. Jin, and D. J. Hill, "Composite load modeling via measurement approach," *IEEE Trans. Power Syst.*, vol. 21, no. 2, pp. 663–672, May 2006.
[10] C. Wang, Z. Wang, J. Wang, and D. Zhao, "Robust time-varying parameter identification for composite load modeling," *IEEE Trans. Smart Grid*, vol. 10, no. 1, pp. 967–979, Jan. 2019.
[11] L. Dzafic, M. Glavic, and S. Tesnjak, "A component-based power system model-driven architecture," *IEEE Trans. Power Syst.*, vol. 19, no. 4, pp. 2109–2110, Nov. 2004.
[12] A. Gaikwad, P. Markham, and P. Pourbeik, "Implementation of the WECC composite load model for utilities using the component-based modeling approach," in *Proc. IEEE/PES Transmiss. Distrib. Conf. Expo. (T&D)*, May 2016, pp. 1–5.
[13] I. F. Visconti, D. A. Lima, J. M. C. D. S. Costa, and N. R. D. B. C. Sobrinho, "Measurement-based load modeling using transfer functions for dynamic simulations," *IEEE Trans. Power Syst.*, vol. 29, no. 1, pp. 111–120, Jan. 2014.
[14] F. Hu, K. Sun, A. D. Rosso, E. Farantatos, and N. Bhatt, "Measurement-based real-time voltage stability monitoring for load areas," *IEEE Trans. Power Syst.*, vol. 31, no. 4, pp. 2787–2798, Jul. 2016.
[15] A. Rogovyh, N. Natalinova, A. Spiridonova, and A. Gordynets, "Inspection methods of load-recording device gamma-500,"' in *Proc. Int. Siberian Conf. Control Commun. (SIBCON)*, May 2015, pp. 1–4.
[16] K. Gai, Y. Wu, L. Zhu, L. Xu, and Y. Zhang, "Permissioned blockchain and edge computing empowered privacy-preserving smart grid networks," *IEEE Internet Things J.*, vol. 6, no. 5, pp. 7992–8004, Oct. 2019.
[17] J. Wang, L. Wu, K.-K.-R. Choo, and D. He, "Blockchain-based anonymous authentication with key management for smart grid edge computing infrastructure," *IEEE Trans. Ind. Informat.*, vol. 16, no. 3, pp. 1984–1992, Mar. 2020.
[18] S. Chen, H. Wen, J. Wu, W. Lei, W. Hou, W. Liu, A. Xu, and Y. Jiang, "Internet of Things based smart grids supported by intelligent edge computing," *IEEE Access* vol. 7, pp. 74089–74102, 2019.

[19] P. Regulski, D. S. Vilchis-Rodriguez, S. Djurovic, and V. Terzija, "Estimation of composite load model parameters using an improved particle swarm optimization method," *IEEE Trans. Power Del.*, vol. 30, no. 2, pp. 553–560, Apr. 2015.
[20] S. Yu, S. Zhang, Y. Han, C. Lu, Z. Yu, and X. Zhang, "Fast parameter identification and modeling of electric load based on simplified composite load model," in *Proc. IEEE Power Energy Soc. Gen. Meeting*, Jul. 2015, pp. 1–5.
[21] J. Xie, Z. Ma, K. Dehghanpour, Z. Wang, Y. Wang, R. Diao, and D. Shi, "Imitation and transfer Q-learning-based parameter identification for composite load modeling," *IEEE Trans. Smart Grid*, vol. 12, no. 2, pp. 1674–1684, Mar. 2021.
[22] S. Yu, S. Zhang, and X. Zhang, "A two-step method for online parameter identification of a simplified composite load model," in *Proc. IEEE Innov. Smart Grid Technol. Asia (ISGT-Asia)*, Nov. 2016, pp. 1025–1030.
[23] M. Kelly, "An introduction to trajectory optimization: How to do your own direct collocation," *SIAM Rev.*, vol. 59, no. 4, pp. 849–904, Jan. 2017.
[24] H. Wu, D. Shen, B. Xia, Y. Qiu, Y. Zhou, and Y. Song, "Parametric problems in power system analysis: Recent applications of polynomial approximation based on Galerkin method," *J. Modern Power Syst. Clean Energy*, vol. 9, no. 1, pp. 1–12, 2021.
[25] F. Gao and L. Han, "Implementing the nelder-mead simplex algorithm with adaptive parameters," *Comput. Optim. Appl.*, vol. 51, no. 1, pp. 259–277, Jan. 2012.
[26] S. Son, S. H. Lee, and D.-H. Choi, "Improvement of composite load modeling based on parameter sensitivity and dependency analyses," *IEEE Trans. Power Syst.*, vol. 29, no. 1, pp. 242–250, Jan. 2014.
[27] X. Tian, X. Lii, L. Zhao, Z. Tan, S. Luo, and C. Li, "Simplified identification strategy of load model based on global sensitivity analysis," *IEEE Access*, vol. 8, pp. 131545–131552, 2020.
[28] L. Haoguang, Y. Yunhua, and S. Xuefeng, "Load parameter identification based on particle swarm optimization and the comparison to ant colony optimization," in *Proc. IEEE 11th Conf. Ind. Electron. Appl. (ICIEA)*, Jun. 2016, pp. 545–550.
[29] S. Ganguly and D. Samajpati, "Distributed generation allocation on radial distribution networks under uncertainties of load and generation using genetic algorithm," *IEEE Trans. Sustain. Energy*, vol. 6, no. 3, pp. 688–697, Jul. 2015.
[30] R. Killick, P. Fearnhead, and I. A. Eckley, "Optimal detection of changepoints with a linear computational cost," *J. Amer. Statist. Assoc.*, vol. 107, no. 500, pp. 1590–1598, 2012.
[31] H. Wu, Y. Zhou, S. Dong, and Y. Song, "Probabilistic load flow based on generalized polynomial chaos," *IEEE Trans. Power Syst.*, vol. 32, no. 1, pp. 820–821, Jan. 2017.
[32] D. Shen, H. Wu, B. Xia, and D. Gan, "Polynomial chaos expansion for parametric problems in engineering systems: A review," *IEEE Syst. J.*, vol. 14, no. 3, pp. 4500–4514, Sep. 2020.
[33] Y. Xu, L. Mili, and J. Zhao, "Probabilistic power flow calculation and variance analysis based on hierarchical adaptive polynomial chaos-ANOVA method," *IEEE Trans. Power Syst.*, vol. 34, no. 5, pp. 3316–3325, Sep. 2019.
[34] X. Ma and N. Zabaras, "An adaptive hierarchical sparse grid collocation algorithm for the solution of stochastic differential equations," *J. Comput. Phys.*, vol. 228, no. 8, pp. 3084–3113, May 2009.
[35] R. A. Waltz, J. L. Morales, J. Nocedal, and D. Orban, "An interior algorithm for nonlinear optimization that combines line search and trust region steps," *Math. Program.*, vol. 107, no. 3, pp. 391–408, 2006.
[36] J. C. Lagarias, J. A. Reeds, M. H. Wright, and P. E. Wright, "Convergence properties of the Nelder–Mead simplex method in low dimensions," *SIAM J. Optim.*, vol. 9, no. 1, pp. 112–147, 1998.

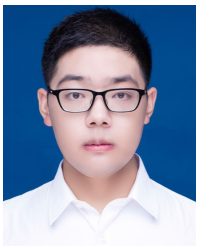

YUJIE CHEN received the B.E. degree in electrical engineering from Zhejiang University, Hangzhou, China, in 2020, where he is currently pursuing the M.S. degree in electrical engineering. His research interest includes power system load modeling.

HAO WU (Member, IEEE) received the Ph.D. degree in electrical engineering from Zhejiang University, Hangzhou, China. He has been with the Faculty of Zhejiang University, since 2002. His current research interests include power system operation and stability, uncertainty analysis, and load modeling.

YIMING SHEN received the M.S. degree in electrical engineering from Zhejiang University, Hangzhou, China, in 2022. Her research interest includes power system load modeling.

XIAN MENG is currently a Senior Engineer with Electric Power Research Institute of Yunnan Power Grid Company. His research interest includes power system analysis.

PING JU (Senior Member, IEEE) received the B.Eng. and M.Sc. degrees in electrical engineering from Southeast University, Nanjing, China, in 1982 and 1985, respectively, and the Ph.D. degree in electrical engineering from Zhejiang University, Hangzhou, China, in 1988. He is currently a Chair Professor with Zhejiang University. His current research interests include load modeling, flexible load dispatch, and integrated energy systems.